High Performance Polysodium Acrylate Superabsorbents Utilizing Microfibrillated Cellulose to Augment Gel Properties

High performance polysodium acrylate superabsorbents utilizing microfibrillated cellulose to augment gel properties

Mikael Larsson[a]*, Mats Stading[b] and Anette Larsson[a]

[a] Department of Chemical and Biological Engineering, Chalmers University of Technology, 41296 Göteborg, Sweden. Fax: +46 31 772 34 18; Tel: +46 317721000, E-mail: mikael.larsson@chalmers.se, anette.larsson@chalmers.se

[b] Structure and Material Design, SIK – The Swedish Institute for Food and Biotechnology and Department of Materials and Manufacturing Technology, Chalmers University of Technology, PO Box 5401, 40229 Göteborg, Sweden. Fax: +46 31833782, Tel: +46 105166637, E-mail: mats.stading@sik.se

* Corresponding author

E-mail: mikael.larsson@chalmers.se

Tel.: +46 31 772 34 11

Fax: +46 31-772 34 18

Abstract

Microfibrillated cellulose was utilized at low concentrations as a filler material, added prior to free radical polymerization, in crosslinked superabsorbent polysodium acrylate hydrogels. The effect of microfibrillated cellulose concentration on equilibrium swelling, shear modulus after synthesis and shear modulus at equilibrium swelling was studied at different degree of crosslinking. For the characterisation of the microfibrillated cellulose optical microscopy, atomic force microscopy and transmittance analysis were used. The shear modulus of the samples was determined using uniaxial compression analysis. The swelling of the gels was determined using classical gravimetrical measurements. It was found that microfibrillated cellulose was highly efficient in increasing the shear modulus of the gels. Furthermore, the microfibrillated cellulose was found to have the same effect on the swelling and shear modulus at equilibrium swelling as the same mass of the conventional covalent crosslinker MBA, while in fact improving the fracture resistance of the gels. In conclusion, microfibrillated cellulose shows great potential as an additive to enhance the performance of soft materials

Keywords: Superabsorbents, MFC, Hydrogels.

Introduction

Hydrogels are materials that have been and currently are subjected to extensive studies due to their importance and future potential in a wide range of applications. They can be used as drug delivery systems, as absorbents in hygiene products, as cell scaffolds in medicine and biology, in sensing systems as the responsive material, among other applications (1-4). Polyacrylic acid (PAA) neutralized with sodium ions is commonly used in superabsorbent hydrogels. The effect of the sodium ions is to increase the osmotic pressure, and thus the swelling capacity of the gels (5). The performance of hydrogels in different applications is highly dependent on the shear modulus, the resistance to fracture and the water absorbance capacity among other properties. These properties are strongly affected by the degree of crosslinking. It has been shown that for PAA the equilibrium degree of swelling decreases (6, 7) and the shear modulus increases (8) with increasing crosslinking, as expected from theory (9).

Much research has been performed on different fillers, both in dry polymer materials and in hydrogels, in order to enhance material properties. There are today several theories available to explain and predict the effect of fillers on the sample properties. Depending on the nature of the filler and the matrix two extreme cases can be identified: (i) no interaction is present between the gel matrix and the dispersed particles, resulting in a decreased modulus for small deformations, or (ii) a strong interaction is present, resulting in an increase in the modulus at small deformations (10). As early as 1944, Smallwood presented a simple approach based on hydrodynamic theories to describe the effect of spherical particles in a rubbery matrix with perfect adhesion between the rubber matrix and the filler. The following expression was formulated for the shear modulus G of such composite materials (11):

$$G = G_m\left(1 + 2.5\phi\right) \qquad (1)$$

This is known as the Einstein-Smallwood formula, where G_m is the shear modulus of the matrix, and ϕ is the volume fraction of filler. The equation is valid under the following conditions: The filler particles are spherical, there is complete adhesion between rubber and filler, the elongation is small, the filler is completely dispersed, the volume loading is small and the filler particles are sufficiently large that the molecular structure of the rubber may be neglected (11). Later, by utilizing the equation for viscosity increase in concentrated suspensions stipulated by Guth and Gold (12) Eq. 1 was extended to higher concentrations as (13-15):

$$G = G_m\left(1 + a\phi + b\phi^2\right) \qquad (2)$$

where a and b are geometry dependent coefficients, for spherical geometry of the fillers and a homogenous dispersion they take the values 2.5 and 14.1, respectively. For a heterogeneous dispersion containing clusters, the values of the coefficients are different, but the validity of Eq. 2 remains (13). It has also been shown by Huber and Vilgis that for low concentrations of rigid filler particles with fractal structure, the reinforcing effect shows linear dependence on the volume fraction of filler and weak dependence on the particle geometry. However, above a critical overlap concentration the reinforcement's dependence on volume fraction of filler is to the power of four and there is a strong dependence on particle geometry (16).

In many cases the effect of a filler on the properties of a composite material can not be explained simply by hydrodynamic theories. It is known that polymers tend to adsorb to surfaces. In particular, polymers would adsorb to surfaces with a roughness on the length scale of a polymer coil (13). This is due to the conformational entropy earned by adsorbing as a coil, rather than as a stretched chain on a flat surface. The adsorption may even be regarded as irreversible for strongly interacting polymer-particle systems (17). In some cases the adsorption of polymer chains on the filler particles will in fact dominate the reinforcement, making the hydrodynamic contribution negligible (13).

Another way in which a polymer matrix can strongly interact with filler particles is through covalent bonds by coupling agents or grafting to the filler surface (18-20). The covalent bonds between the polymer network and fillers have been reported to improve composite properties more than simple mixing with the fillers. Both adsorption and chemical bonding of polymer chains on filler particles will effectively act as junction points in the polymer network, contributing to the shear modulus of the material. It is obvious that the reinforcing effect due to surface adsorption and chemical bonds is strongly dependent on the total area and spatial distribution of filler. Indeed it has been shown both experimentally (17, 21-24) and theoretically (25) that for nanocomposites the shear modulus is significantly enhanced even for small volume fractions of filler. This is not surprising; consider e.g. the case with a volume fraction 0.01 of spherical filler with 50 nm diameter. The total surface area of the fillers would be ~ 1.2 m^2 in 1 cm^3 of sample, and the average distance between randomly dispersed particles ~ 140 nm. Individual filler particles can thus be connected over large distances, as compared to their sizes, through the polymer network (17).

Lately, in the light of the emerging field of conscious nano science, many studies have investigated the influence of different nano sized fillers on the properties of hydrogels. The studied characteristics include mechanical properties (22, 23, 25, 26), swelling (27-29) properties, or both (30, 31), only to give some examples of articles on the subject.

Cellulose nanofibers, also called microfibril cellulose in some literature, or nanocrystalline cellulose are promising biological alternatives to commonly used inorganic micro- nanofillers (32). There are several different preparation methods and cellulose raw materials that affect the structural properties and surfaces charges of the microfibril or nanofibril cellulose product. Typical dimensions for wood based nanofibers are some nanometers in diameter and some hundreds of nanometers, and even up to micrometers, in length (32-34), whilst approximately spherical nanocrystals have been shown to have a

diameter of 10's – 100's of nm (35-38). It has been shown that the addition of a small amount of cellulose nanofibers can cause a significant increase of the Young's modulus for the composite material as compared to the reference sample (26, 32, 39-42). Furthermore, there are several reports on the grafting of molecules and polymers onto cellulose (19, 32, 43-45). The grafting of the polymer network to nano-dimensioned cellulose filler should, as discussed above, significantly influence the material properties.

There have been studies on the preparation of hydrogels based on cellulose nanofibers (46, 47) and on the rheology during gelation of polysodium acrylate gels with rather large, micrometer dimensioned, microfibril cellulose used as filler (42). However, to the authors' knowledge, there is to date no study of the effect of cellulose with sub micrometer dimensions, or of commercially available microfibrillated cellulose (MFC), as filler in a superabsorbent hydrogel matrix.

This study intended to elucidate the effects of low concentrations of commercially available MFC, utilized as filler, on the mechanical and swelling properties of crosslinked superabsorbent hydrogels swollen in saline solution. The superabsorbent matrix of choice was polysodium acrylate and the methods used were; optical microscopy, atomic force microscopy (AFM), transmittance analysis, uniaxial compression analysis and traditional gravimetrical measurements of absorbed water.

Experimental

Materials

The following chemicals were of analytical grade and were used as received; acrylic acid [AA] (Fluka, Belgium), N,N'-methylenebisacrylamide [MBA] (Sigma-Aldrich, Germany), sodium chloride (Sigma-Aldrich, Germany), sodium hydroxide (Sigma-Aldrich, Germany),

potassium persulfate [KPS] (Sigma-Aldrich, Germany). Micro fibrillated cellulose [MFC] was bought from the Paper and Fibre Research Institute PFI, Norway. Used H_2O was of Milli-Q grade.

Characterisation of the microfibrillated cellulose suspension

Both untreated and filtered MFC suspension was characterized using light microscope and AFM. Filtered MFC suspension was further characterised by transmittance analysis.

Filtered MFC suspension was prepared using a 25 mm syringe filter with 0.2 µm nylon membrane (VWR), previously washed with 30 ml of H_2O.

For the light microscopy analysis an Olympus BH2 research microscope with a Microscope digital camera system DP12 (Olympus) was used in transmission mode. For untreated MFC suspension images were recorded for concentrations of 0.03 and 0.8 % w/v, placed between a standard microscope glass slide and a cover slip. For filtered suspension images were recorded on samples dried at room temperature on a standard microscopy glass slide, utilizing filtered and dried H_2O as controls.

Untreated MFC suspension samples to be analysed in AFM were prepared by diluting the suspension to MFC concentrations of 0.16, 0.016 and 0.0016 % w/v. For both untreated and filtered MFC one drop of sample was added to a freshly cleaved mica chip and was allowed to dry at room temperature, for the filtered sample filtered water was used as control. The AFM analysis was performed using a Digital Instrument Nanoscope IIIa with a type G scanner (Digital Instrument Inc.). The cantilever used was a Mikro Masch silicon cantilever NSC 15. The AFM was operated at a resonance frequency of about 330 kHz in tapping mode, the scan rate was 1 Hz and the measurements were performed in air.

For transmittance analysis of filtered MFC suspension the extinction of light passed through the sample in a quarts cuvette was recorded as a function of wavelength in the interval 200-800 nm using a Cintra 40 spectrophotometer (GBC), filtered H_2O was used as a control.

Synthesis

Hydrogels containing 25 % w/v AA with MBA:AA ratios ranging from 0 to 0.05 and MFC concentrations ranging from 0 to 0.75 % w/v were synthesized by free radical copolymerization as follows: AA was drop wise neutralized to 60 mol% with NaOH. The neutralized AA was mixed with MBA, KPS, H_2O and MFC suspension (1.6 % w/v). KPS was used in a concentration of 21 mM, the amounts of MBA and MFC suspension were added according to desired final concentrations and H_2O was added to reach the final volume. All of the mixing was performed on ice during stirring. After mixing the samples were bubbled with N_2 gas under stirring while kept on ice for 30 minutes, this to remove O_2 from the samples. The samples were then immediately transferred to 7x40 mm autosampler vials (NTK KEMI), which were placed in a water bath at 70 °C for 6 h for the synthesis solution to polymerize. Finally the samples were allowed to settle over night at room temperature before breakage of the vials and further analysis.

Mechanical measurements

The gels were cut into cylinders intending an aspect ratio > 1.5. However, on rare occasions a smaller aspect ratio was acquired due to removal of rough sample ends. Uniaxial compression tests were performed in order to determine the shear modulus *G* of the different samples. The samples were compressed at 0.1 $mm \cdot s^{-1}$ and the resulting force was recorded using a TA-

HDi® (Stable Microsystems), with a load cell capacity of 5 kg. The compression probe used was a 25 mm cylindrical aluminium probe (Stable Microsystems). Measurements were performed at 20 ± 0.5 °C. For the uniaxial compression of Gaussian chains the following equation is valid (48):

$$P = G\left(\alpha - \alpha^{-2}\right) \quad (3)$$

where P is the pressure, G is the shear modulus and α is the ratio deformed length to initial length.

For deformation ratios up to 20 % the shear modulus was determined as the slope of the linear region in the graph P versus (α-α^{-2}), similar to previous works (49-53). The non linear data for low strains was discarded as it is derived from imperfect geometries of the sample ends (51, 53). The compressive strength of the samples was calculated as:

$$\sigma = F / A \quad (4)$$

where F is the force at fracture and A is the area at fracture, calculated based on the assumption of constant volume (48) as:

$$A = \frac{A_0}{\alpha_f} \quad (5)$$

where A_0 is the initial area and α_f is the deformation ratio at fracture.

Swelling analysis

The samples were prepared for swelling by cutting of and discarding the uppermost part of the cylinders and recording their weights w_0. The swelling experiments were conducted in 900 ml of 0.90 % w/v NaCl at 20 ± 0.5 °C. After one week the samples were considered to have reached equilibrium swelling as no further mass uptake could be detected. The equilibrium

weight w_{eq} was recorded. Assuming a yield of 100% from the synthesis as done by others (54, 55), the dry weights of the samples were calculated from the masses of the components in the synthesis mixture and the weight ratio between the initial weight w_0 of the samples and the synthesis mixture, so that:

$$m_{dry} = m_{AA} + m_{NaA} + m_{MBA} + m_{MFC} \quad (6)$$

where m_{dry} is the theoretical dry weight of the sample, m_{AA} is the mass of AA, m_{NaA} is the mass sodium acrylate, m_{MBA} is the mass MBA and m_{MFC} is the mass of MFC in the sample. The swelling degree Q was then calculated as:

$$Q = \frac{\left(w_{eq} - m_{dry}\right)}{m_{dry}} \quad (7)$$

Results and discussion

Characterisation of microfibrillated cellulose suspension

The structural composition of MFC can vary greatly depending on the source of the original cellulose fibers and the manufacturing process. In order to elucidate the structural components of the MFC suspension in question visual inspection, followed by optical microscopy, AFM and transmittance analysis were performed on the untreated suspension and on suspension filtered through a filter with 0.2 µm pores. During the visual inspection of the untreated suspension it was noted that small amounts of fiberous structures could be detected with the naked eye and that the suspension appeared opaque. The filtered suspension appeared completely transparent.

Optical microscopy of wet MFC suspension revealed a highly heterogeneous suspension on the detectable length scale, as can be seen in the exemplifying images in Fig. 1a. Filtered and subsequently dried MFC suspension left a film like aggregate over the whole

area covered by the drop prior to drying. In the aggregate area structures of varying size could be seen, many with clear directionality and even fractal like structures. It was found that size and shape of the structures varied between samples. This was probably due to different concentrations and size distributions of MFC in the samples after filtration and due to variations in drying between samples. Exemplifying images can be seen in Fig. 1b. The controls with filtered water did not show any observable structures and only negligible aggregate, probably being an artefact from the filtration or the drying. The large aggregate formation and the formed structures from MFC suspension filtered through a 0.2 µm filter clearly indicates the presence of structures with sizes on the nano-scale.

AFM analysis of the MFC suspension revealed that the MFC contained a large amount of nanoparticles, thought to be cellulose nanocrystals, as well as larger fibers and fiberous structures. An exemplifying image showing individual nanoparticles, fibers and larger fiberous structures is given in Fig. 2a. Typical dimensions in the z-direction were found to be about 2-5 nm for nanoparticles and individual fibers and about 30-60 nm for fiber bundles. However, the structures observed varies greatly between locations in the dried samples, as such there will be structures present falling outside the mentioned intervals. The observed nanoparticles had diameters in the xy-plane of 10's of nanometers, this is similar to diameters reported by others for spherical cellulose nanocrystals (35, 37, 38). The exact diameters of the nanoparticles are not speculated upon. This since the AFM tip is known to give artifacts in the xy-plane (33). However, the AFM has very high precision in the z-direction, and it can be concluded that the structure of the thought to be cellulose nanocrystals is somewhat flattened.

AFM analysis of the filtered MFC suspension and the filtered water control revealed that the filtered MFC contained nanoparticles and fibers (Fig. 2b and c). The dimensions in the z-direction ranged from about 1–20 nm for the nanoparticles and 1-2 nm for the fibers. As stated earlier, structures falling outside the mentioned intervals should also be present. The

AFM analysis of the water control revealed that a thin film with pores had been formed upon drying of the sample (result not shown). Thus, the dark areas, corresponding to cavities, in Fig. 2b and c are derived from this film, and are not associated with the MFC suspension.

Transmittance analysis of the filtered suspension showed an increasing extinction with decreasing wavelength. The transmittance through a medium containing particles can be described by the Beer Lambert law, replacing the extinction coefficient with a scattering coefficient (56), with the current notation:

$$A = \alpha_{sca} l \qquad (8)$$

where A is the absorbance, l is the distance through the medium and α_{sca} is the scattering coefficient, which for Rayleigh scattering from small size particles is inversely proportional to the fourth power of the wavelength (57).

In order to evaluate if the extinction was due to Rayleigh scattering the absorbance was plotted versus λ^{-4}. In Fig. 3 it can be seen that extinction is indeed relatively proportional to λ^{-4}.

Taking into account the results from optical microscopy of filtered suspension, AFM and transmittance studies, it is concluded that the MFC suspension contains rather large amounts of structures having sizes on the nano scale. The differences in the structures observed in the AFM analysis of the 10, 100 and 1000 times diluted samples, as well as the structures observed for filtered and subsequently dried MFC using optical microscopy, indicates that upon drying the nanoparticles aggregate into larger structures in a concentration dependent manner. Aggregation of cellulose nanocrystals into structures upon drying has been previously reported by Wang et al. (35).

Based on the characterisation it is recognized that the used MFC is highly heterogeneous; containing particles, fibers and fiber clusters, ranging from nanometers to hundreds of micrometers in size.

Sample preparation

In order to evaluate the effect of the MFC utilized as a filler material, on the mechanic and swelling properties of the hydrogels, two series of samples were studied. The first was to evaluate the effect of the amount of MFC on the properties in a fixed surrounding matrix. This set contained hydrogels with a fixed molar ratio of the crosslinker N,N'-methylenebisacrylamide (MBA) to acrylic acid (AA) of 0.005 and MFC concentrations ranging from 0 to 2.5 % per dry weight of the samples.

The second set was to elucidate the influence of a fixed amount of MFC when the modulus of the surrounding matrix was changed. This set contained hydrogels with MBA:AA ratios ranging from 0 to 0.05 and a MFC concentration of 1.2 % per dry weight. As references, samples without MFC were prepared at each specified MBA:AA ratio.

After synthesis it was observed that the MFC containing gels were increasingly opaque with increasing MFC concentration, as expected since this was also the case both for the MFC suspension and the pre-polymerization mixture. The samples without MFC displayed a fully transparent appearance.

Shear modulus after synthesis

The shear modulus determined from the uniaxial compression analysis showed that the reinforcing effect in a fixed matrix with a MBA:AA of 0.005 increased with increasing concentration of MFC. First a larger increase was observed for a low amount of added MFC,

followed by a rather linear increase with increasing MFC concentration, as shown in Fig. 4a. From Eq. 2, it is seen that the increase in modulus should have an approximately linear dependence on the volume fraction of filler for low filler concentrations and a quadratic dependence for high concentrations according to hydrodynamic theories. As such, it can be concluded that the observed reinforcing effect can not be explained by hydrodynamic theories alone. Even if neglecting the sample without MFC and the large initial increase in modulus, focusing only on the linear region, the reinforcement is much more effective than expected for traditional hard fillers. By extrapolating the linear region to a filler concentration of zero to approximate the surrounding matrix modulus and fitting the data to Eq. 1 or 2, the geometry coefficient was found to have a value of approximately 40. That is, in the linear region the increase of modulus with increasing volume fraction of filler is 16 times larger than the value of 2.5 expected for traditional hard fillers with spherical geometry.

In the case with a fixed MFC concentration of 1.2 % per dry weight and varying MBA:AA ratio, it can be seen in Fig. 4b that the shear modulus is proportional to the amount of crosslinker for samples both with and without MFC. This is expected from a crosslinked polymer network according to theory (48). Furthermore, an increase in the modulus can be seen for the MFC containing samples when compared to those with no MFC. Interestingly, it was found that the increase in modulus was small for the samples with no or low amount of covalent crosslinker (MBA:AA ratios of 0 and 0.001). Furthermore, the increase in modulus relatively to that of corresponding samples without MFC exhibited a maximum for a MBA:AA ratio of 0.005. From the results, it can be concluded that the reinforcing mechanism is complex.

Equilibrium swelling and shear modulus.

In order to establish the effect of MFC on equilibrium swollen gels the samples were submerged in 0.9 % NaCl solution. The specified ionic strength was chosen because of the biological relevance and because superabsorbents swollen in de-ionized water commonly fracture during swelling.

The swelling studies revealed, as expected, that the equilibrium swelling decreased with both increasing content of MBA and MFC. Surprisingly, when plotting the equilibrium swelling degree Q_e versus the combined percentage of MBA and MFC per dry weight (Fig. 5a), it was found that the equilibrium swelling degree was relatively independent of the MBA:MFC weight ratio, rather depending only on the combined mass of MBA and MFC added to the synthesis solution. A minor deviation from the observation may be seen for the point that corresponds to a MBA:AA ratio of 0.001 with MFC (indicated in Fig. 5a).

The shear modulus after swelling of the samples displayed an increase with increasing mass of both MBA and MFC, shown in Fig. 5b. As for the equilibrium swelling of the samples, the effect on the shear modulus was found to be relatively independent of whether MBA:MFC weight ratio, as long as the combined mass was the same.

The decrease in swelling and increase in shear modulus with crosslinking is to be expected according to theory on crosslinked gels (9). However, to elucidate the actual performance of the MFC containing gels as compared to that of gels with only conventional crosslinker, it is necessary to investigate the shear modulus at a given equilibrium swelling $G(Q_e)$. It has been previously stated that for swollen polymer networks, where only the degree of crosslinking changes, the shear modulus at equilibrium can be expressed, with the current notation, as (58-60):

$$G(Q_e) = AQ_e^{-m} \qquad (9)$$

where A and m are material and solvent dependent coefficients. Indeed, when making a plot of log G versus log Q_e (Fig. 5c), a linear relationship is acquired. From linear regression of the data the value $m = 2.4$ is acquired. For the case of a good solvent, the theoretical value of m is predicted to be 2.25 (58, 59) and has been reported as 2.3 (61) and 2.4 (62) in experimental studies. It seems from the data in Fig. 5c that MFC containing samples with a MBA:AA ratio of 0.001 (indicated in the figure) has a larger $G(Q_e)$, as compared to samples without MFC with similar Q_e. To substantiate this observation, being aware that the differences could be due to variations between syntheses, additional samples were synthesised and analysed. The further analyses were performed on the swelling and shear modulus of samples with a MBA:AA ratio of 0.005, corresponding to a MBA content of 0.89 % per dry weight, without MFC and on samples with a MBA:AA ratio of 0.001, corresponding to a MBA content of 0.18 % per dry weight, with 1.2 % MFC per dry weight. Those compositions were chosen as they exhibited similar Q_e's.

The results, $G(Q_e)$, shown in Fig. 5d indicates that there may be an improvement for MFC containing samples. However, it is difficult to statistically verify the improvement due to rather large variations, both in G and Q_e between syntheses. As such we dare not state that there is an actual increase in $G(Q_e)$ for MFC containing samples. The results do show that under the current conditions and compositions, the traditional covalent crosslinker MBA can to large parts be replaced with the same mass of MFC. The composite samples exhibiting similar Q_e and at least as good $G(Q_e)$ as samples with only MBA.

The large effect of MFC on Q_e and $G(Q_e)$ must be attributed to strong interactions between the MFC filler particles and the polymer network. Since the samples were prepared by free radical polymerization initiated with KPS and it is known that grafting onto cellulose can be performed using redox initiated free radical processes (45), it seems likely that the polymer network was grafted onto the MFC during the synthesis. However, polymers are also

known to strongly adsorb to surfaces (13) and the mechanism of polymer-MFC interaction is probably a combination of covalent and physical bonds. It is recognized that the mechanism of the reinforcement is complex, especially since the effect of MFC as compared to MBA is totally different between samples after synthesis and after equilibrium swelling.

Fracture on compression

During the uniaxial compression measurements it was possible to determine the strain $\varepsilon_f = (l_0 - l) / l_0$ at which the gels fractured for samples with MBA:AA ratios of 0.025 and 0.05, containing 0 or 1.2 % MFC per dry weight. For samples with lower amount of crosslinker this was not possible as the gels in many cases squeezed away from the compression rather than fractured. It was found that for samples containing MFC the stress at fracture (compressive strength) σ_f was increased without decreasing the strain at fracture, compared to corresponding samples without MFC (Table 1).

The samples analysed after synthesis are directly comparable as they have the same volume fraction of polymer. The data in Table 1 clearly shows on improved gel properties for MFC containing samples, with regard to fracture. The sample with MBA:AA ratio of 0.025 and MFC displayed both the best deformability and the largest compressive strength. However, due to the rather large variation between measurements, the sample with MBA:AA ratio of 0.05 and MFC could in fact be the one having the largest compressive strength. For the swollen samples one needs to be aware that the volume fraction of polymer differs about 11% between samples with and without MFC containing the same amount of MBA. Despite the difference in swelling between samples it can be concluded that MFC is increasing the performance of the gels after swelling, with regard to fracture. The sample with MBA:AA ratio of 0.025 and MFC displayed a deformability equal to that of the sample with the same

amount of MBA without MFC and better than that of the sample with MBA:AA ratio of 0.05 without MFC, while it seemingly exhibited a larger compressive strength than both.

The increase in compressive strength is not surprising since it has been long known that fillers can have that effect (63). However, what is beneficial is that the increase takes place without decreasing the strain ε_f at which the fracturing takes place. Simple theory predicts that for a hard filler composite the strain at which fracture occurs should always decrease (63). Furthermore, the samples without MFC in this study become more prone to fracture as the modulus is increased using conventional crosslinker. Thus, it can be concluded that by using MFC at a concentration of 1.2 % per dry weight, the shear modulus can be improved without worsening the deformation properties with regard to fracture, in contrast to what would be expected for traditional hard fillers and what is observed with the traditional crosslinker MBA for the samples in this study.

Conclusion

In this study it has been shown that commercially available microfibrillated cellulose (MFC) with structural content ranging in size from nano to micro, is highly efficient, with regard to reinforcement, when utilized as a filler in superabsorbents composed of polyacrylic acid neutralized with NaOH, prepared by free radical copolymerization. The highly efficient reinforcement and the deviance from hydrodynamic theories clearly show that the mechanism is more complex than suggested by hard filler theory, indicating strong interaction between the MFC and the polymer network. Possible explanations for the strong interaction are adsorption of the polymer network onto the MFC and grafting of the polymer network onto the MFC during the polymerization reaction. A surprising finding was that the MFC had the same effect on equilibrium swelling and shear modulus in the swollen state as the same mass of the conventional crosslinker MBA, while at the same time improving the samples'

resistance to fracture. The results clearly indicate that MFC holds great potential as a biologic reinforcing material in the area of soft materials, in some cases possibly replacing reactive conventional crosslinkers. Future scopes would be to perform toxicological studies of MFC to elucidate the potential as a reinforcing filler material in biological applications, to perform studies utilizing MFC with more well defined structural content to in detail elucidate how different MFC geometries and sizes will influence the composite properties and to in detail investigate the mechanism of polymer-MFC interactions under different conditions in different systems.

Acknowledgements

We want to thank Dr. Stefan Gustafsson and Dr. Eva Olsson at The Department of Applied Physics, Chalmers University of Technology, for valuable discussions and Anders Mårtensson at The Department of Chemical and Biological Engineering, Chalmers University of Technology, for his help with the AFM image analysis. This work was performed within the VINN Excellence Centre SuMo Biomaterials (Supermolecular Biomaterials – Structure dynamics and properties). The financial support from the Centre is gratefully acknowledged. Further financial support was acquired from the Swedish Research Council and from Chalmers Bioscience Program, Chalmers University of Technology.

References

1. Schacht, E.H. (1984) Hydrogel drug delivery systems physical and ionogenic drug carriers. Recent Adv. Drug Delivery Syst., Proc. Int. Symp.:259-278.
2. Hendrickson, G.R.; Andrew Lyon, L. (2009) Bioresponsive hydrogels for sensing applications. Soft Matter 5(1):29-35.
3. Peppas, N.A.; Hilt, J.Z.; Khademhosseini, A.; Langer, R. (2006) Hydrogels in biology and medicine: from molecular principles to bionanotechnology. Adv. Mater. 18(11):1345-1360.
4. Buchholz, F.L.; Graham, A.T. Editors (1998). Modern Superabsorbent Polymer Technology; John Wiley & Sons Inc.: New York, USA.
5. Tong, Z.; Liu, X. (1993) Swelling equilibria and volume phase transition of partially neutralized poly(acrylic acid) gels. Eur. Polym. J. 29(5):705-709.
6. Jovanovic, J.; Adnadjevic, B. (2007) Influence of poly(acrylic acid) xerogel structure on swelling kinetics in distilled water. Polym. Bull. 58(1):243-252.
7. Yang, M.; Song, H.; Zhu, C.; He, S. (2007) Radiation synthesis and characterization of polyacrylic acid hydrogels. Nucl. Sci. Tech. 18(2):82-85.
8. Yazici, I.; Okay, O. (2005) Spatial inhomogeneity in poly(acrylic acid) hydrogels. Polymer 46(8):2595-2602.
9. Flory, P.J., Principles of Polymer Chemistry; Cornel Univ. Press: New York, USA
10. Van Vliet, T. (1988) Rheological properties of filled gels. Influence of filler matrix interaction. Colloid. Polym. Sci. 266(6):518-524.
11. Smallwood, H.M. (1944) Limiting law of the reinforcement of rubber. J. Appl. Phys. 15:758-766.

12. Guth, E.; Gold, O. (1938) Hydrodynamical theory of the viscosity of suspensions. Physical Review 53:322.

13. Vilgis, T.A.; Heinrich, M.; Heinrich, G. (1995) Crosslinked polymer blends: theoretical problems from rubber physics to technology. Kautsch. Gummi Kunstst. 48(5):323-335.

14. Heinrich, G.; Kluppel, M.; Vilgis, T.A. (2002) Reinforcement of elastomers. Curr. Opin. Solid State Mater. Sci. 6(3):195-203.

15. Guth, E. (1945) Theory of filler reinforcement. J. Appl. Phys. 16:20-25.

16. Huber, G.; Vilgis, T.A. (2002) On the Mechanism of Hydrodynamic Reinforcement in Elastic Composites. Macromolecules 35(24):9204-9210.

17. Zhang, Q.; Archer, L.A. (2002) Structure and rheology of poly(ethylene oxide)/silica nanocomposites. Langmuir 18(26):10435-10442.

18. Liu, Q.; de Wijn, J.R.; Van Blitterswijk, C.A. (1998) Composite biomaterials with chemical bonding between hydroxyapatite filler particles and PEG/PBT copolymer matrix. J. Biomed. Mater. Res. 40(3):490-497.

19. Bledzki, A.K.; Gassan, J. (1999) Composites reinforced with cellulose based fibres. Prog. Polym. Sci. 24(2):221-274.

20. Rothon, R.N. Editor (2003). Particulate-Filled Polymer Composites. 2nd Ed; Rapra Technology Limited: Shrewsbery, United Kingdom.

21. Zebrowski, J.; Prasad, V.; Zhang, W.; Walker, L.M.; Weitz, D.A. (2003) Shake-gels: shear-induced gelation of laponite-PEO mixtures. Colloids Surf., A 213(2-3):189-197.

22. Haraguchi, K.; Li, H.-J. (2006) Mechanical Properties and Structure of Polymer-Clay Nanocomposite Gels with High Clay Content. Macromolecules 39(5):1898-1905.

23. Agrawal, S.K.; Sanabria-DeLong, N.; Tew, G.N.; Bhatia, S.R. (2008) Nanoparticle-Reinforced Associative Network Hydrogels. Langmuir 24(22):13148-13154.

24. Otsubo, Y.; Watanabe, K. (1990) Rheological studies on bridging flocculation. Colloids Surf. 50:341-352.

25. Surve, M.; Pryamitsyn, V.; Ganesan, V. (2006) Polymer-bridged gels of nanoparticles in solutions of adsorbing polymers. J. Chem. Phys. 125(6):064903/064901-064903/064912.

26. Orts, W.J.; Shey, J.; Imam, S.H.; Glenn, G.M.; Guttman, M.E.; Revol, J.-F. (2005) Application of Cellulose Microfibrils in Polymer Nanocomposites. J. Polym. Environ. 13(4):301-306.

27. Zhang, J.; Zhang, K.; Wang, A. (2008) Study on superabsorbent composites XVII. Preparation and characterization of poly(acrylic acid)/attapulgite/Na-montmorillonite superabsorbent composites. e-Polymers:No pp given.

28. Costantini, A.; Luciani, G.; Annunziata, G.; Silvestri, B.; Branda, F. (2006) Swelling properties and bioactivity of silica gel/pHEMA nanocomposites. J. Mater. Sci. Mater. Med. 17(4):319-325.

29. Ma, Y.; Liu, Y.; Jiang, Y.; Yu, H.; Zhu, M. (2007) Novel rapid response clay/poly(N-isopropylacrylamide) nanocomposite hydrogels by post treatment with HCl solution. e-Polymers:No pp given.

30. Tong, X.; Zheng, J.; Lu, Y.; Zhang, Z.; Cheng, H. (2007) Swelling and mechanical behaviors of carbon nanotube/poly(vinyl alcohol) hybrid hydrogels. Mater. Lett. 61(8-9):1704-1706.

31. Haraguchi, K. (2007) Nanocomposite gels: new advanced functional soft materials. Macromol. Symp. 256(Functional and Biological Gels and Networks: Theory and Experiment):120-130.

32. Siró, I.; Plackett, D. (2010) Microfibrillated cellulose and new nanocomposite materials: a review. Cellulose.

33. Beck-Candanedo, S.; Roman, M.; Gray, D.G. (2005) Effect of Reaction Conditions on the Properties and Behavior of Wood Cellulose Nanocrystal Suspensions. Biomacromolecules 6(2):1048-1054.

34. Henriksson, M.; Henriksson, G.; Berglund, L.A.; Lindstroem, T. (2007) An environmentally friendly method for enzyme-assisted preparation of microfibrillated cellulose (MFC) nanofibers. Eur. Polym. J. 43(8):3434-3441.

35. Wang, N.; Ding, E.; Cheng, R. (2007) Thermal degradation behaviors of spherical cellulose nanocrystals with sulfate groups. Polymer 48(12):3486-3493.

36. Zhang, J.; Elder, T.J.; Pu, Y.; Ragauskas, A.J. (2007) Facile synthesis of spherical cellulose nanoparticles. Carbohydr. Polym. 69(3):607-611.

37. Filson, P.B.; Dawson-Andoh, B.E. (2009) Sono-chemical preparation of cellulose nanocrystals from lignocellulose derived materials. Bioresour. Technol. 100(7):2259-2264.

38. Chang, P.R.; Jian, R.; Zheng, P.; Yu, J.; Ma, X. Preparation and properties of glycerol plasticized-starch (GPS)/cellulose nanoparticle (CN) composites. Carbohydr. Polym. 79(2):301-305.

39. Oksman, K.; Mathew, A.P.; Bondeson, D.; Kvien, I. (2006) Manufacturing process of cellulose whiskers/polylactic acid nanocomposites. Composites Science and Technology 66(15):2776-2784.

40. Morin, A.; Dufresne, A. (2002) Nanocomposites of chitin whiskers from Riftia tubes and poly(caprolactone). Macromolecules 35(6):2190-2199.

41. Choi, Y.; Simonsen, J. (2006) Cellulose nanocrystal-filled carboxymethyl cellulose nanocomposites. J. Nanosci. Nanotechnol. 6(3):633-639.

42. Harini, M.; Deshpande, A.P. (2009) Rheology of poly(sodium acrylate) hydrogels during cross-linking with and without cellulose microfibrils. J. Rheol. 53(1):31-47.

43. Abdel-Razik, E.A. (1997) Aspects of thermal graft copolymerization of methyl methacrylate onto ethyl cellulose in homogeneous media. Polym.-Plast. Technol. Eng. 36(6):891-903.

44. Ghosh, P.; Biswas, S.; Datta, C. (1989) Modification of jute fiber through vinyl grafting aimed at improved rot resistance and dyeability. J. Mater. Sci. 24(1):205-212.

45. Arthur, J.C., Jr. (1982) Free-radical initiated graft polymerization of vinyl monomers onto cellulose. ACS Symp. Ser. (Graft Copolym. Lignocellul. Fibers):21-31.

46. Ono, H.; Shimaya, Y.; Sato, K.; Hongo, T. (2004) H spin-spin relaxation time of water and rheological properties of cellulose nanofiber dispersion, transparent cellulose hydrogel (TCG). Polym. J. 36(9):684-694.

47. Ikkala, O.; Ras, R.H.A.; Houbenov, N.; Ruokolainen, J.; Paakko, M.; Laine, J.; Leskela, M.; Berglund, L.A.; Lindstrom, T.; ten Brinke, G.; Iatrou, H.; Hadjichristidis, N.; Faul, C.F.J. (2009) Solid state nanofibers based on self-assemblies: From cleaving from self-assemblies to multilevel hierarchical constructs. Faraday Discuss. 143(Soft Nanotechnology):95-107.

48. Treloar, L.R.G. (1975). The Physics of Rubber Elasticity. 3rd Ed; Oxford Univ. Press: London, United Kingdom.

49. Knaebel, A.; Rebre, S.R.; Lequeux, F. (1997) Determination of the elastic modulus of superabsorbent gel beads. Polym. Gels Netw. 5(2):107-121.

50. Gundogan, N.; Melekaslan, D.; Okay, O. (2003) Non-Gaussian elasticity of swollen poly(N-isopropylacrylamide) gels at high charge densities. Eur. Polym. J. 39(11):2209-2216.

51. Sayil, C.; Okay, O. (2001) Macroporous poly(N-isopropyl)acrylamide networks: formation conditions. Polymer 42(18):7639-7652.

52. Zrinyi, M.; Horkay, F. (1987) On the elastic modulus of swollen gels. Polymer 28(7):1139-1143.

53. Durmaz, S.; Okay, O. (2001) Inhomogeneities in polyacrylamide gels: position-dependent elastic modulus measurements. Polymer Bulletin 46(5):409-418.

54. Galicia, J.A.; Sandre, O.; Cousin, F.; Guemghar, D.; Menager, C.; Cabuil, V. (2003) Designing magnetic composite materials using aqueous magnetic fluids. J. Phys. Condens. Matter 15(15):S1379-S1402.

55. Ma, P.X.; Elisseeff, J. Editors (2006). Scaffolding in Tissue Engineering; CRC Press: Boca Raton, USA.

56. Schittenhelm, H.; Callies, G.; Berger, P.; Huegel, H. (1996) Investigations of extinction coefficients during excimer laser ablation and their interpretation in terms of Rayleigh scattering. J. Phys. D Appl. Phys. 29(6):1564-1575.

57. Elim, H.I.; Cai, B.; Kurata, Y.; Sugihara, O.; Kaino, T.; Adschiri, T.; Chu, A.-L.; Kambe, N. (2009) Refractive Index Control and Rayleigh Scattering Properties of Transparent TiO2 Nanohybrid Polymer. J. Phys. Chem. B 113(30):10143-10148.

58. De Gennes, P.G. (1979). Scaling Concepts in Polymer Physics; Cornell Univ. Press: Ithaca and London, United Kingdom.

59. Candau, S.; Bastide, J.; Delsanti, M. (1982) Structural, elastic, and dynamic properties of swollen polymer networks. Adv. Polym. Sci. 44(Polym. Networks):27-71.

60. Obukhov, S.P.; Rubinstein, M.; Colby, R.H. (1994) Network Modulus and Superelasticity. Macromolecules 27(12):3191-3198.

61. Zrinyi, M.; Horkay, F. (1984) Studies on mechanical and swelling behavior of polymer networks on the basis of the scaling concept. 5. Crossover effects above and below the q temperature. Macromolecules 17(12):2805-2811.

62. Richards, R.W.; Davidson, N.S. (1986) Scaling analysis of mechanical and swelling properties of random polystyrene networks. Macromolecules 19(5):1381-1389.

63. Nielsen, L.E. (1966) Simple theory of stress-strain properties of filled polymers. J. Appl. Polym. Sci. 10(1):97-103.

Figure Captions

FIGURE 1 Optical microscopy images of MFC suspension.(a) Image of wet 2X diluted suspension using a 10X objective. Insert is 25X diluted using a 100X objective. (b) Image of filtered and dried suspension using a 10X objective. Insert is captured using a 50X objective

FIGURE 2 AFM images of MFC suspension. (a) 10X diluted and subsequently dried, recorded in an area where no macroscopic aggregate was observed using light microscope. z-displacement (range 20 nm) to the left, phase image to the right. (b) and (c) z-displacement images (range 30 nm) of filtered and subsequently dried MFC. The images have been digitally enhanced for clarity, see text for relevant z-displacements of observed structures.

FIGURE 3 Absorbance versus λ^{-4} for filtered MFC suspension, the control with filtered water is sufficiently small to be negligible and is therefore excluded from the figure.

FIGURE 4 Shear modulus after synthesis. (a) For samples with a fixed MBA:AA ratio of 0.005 and varying MFC content. (b) For samples with varying MBA:AA ratios and a fixed MFC content of 1.2 % per dry weight (●) and controls without MFC (○). Error bars indicate min / max values within a synthesis, n = 2

FIGURE 5 Equilibrium swelling (a) and shear modulus at equilibrium swelling (b) for samples with a fixed MBA:AA ratio of 0.005, corresponding to 0.89 % MBA per dry weight, and varying MFC content (x), samples with varying MBA:AA ratios and a fixed MFC content of 1.2 % per dry weight (●) and samples without MFC and varying MBA:AA ratios (○). Error bars indicate standard deviation within a synthesis, n = 3 for swelling and n = 6 for shear

modulus. (c) Plot of log G versus log Q_e for previously described samples. (d) Plot of G versus Q_e for repeated experiments of samples with a MBA:AA ratio of 0.005 without MFC (○) and samples with a MBA:AA ratio of 0.001 and 1.2 % MFC per dry weight (●).

Figures

FIGURE 1

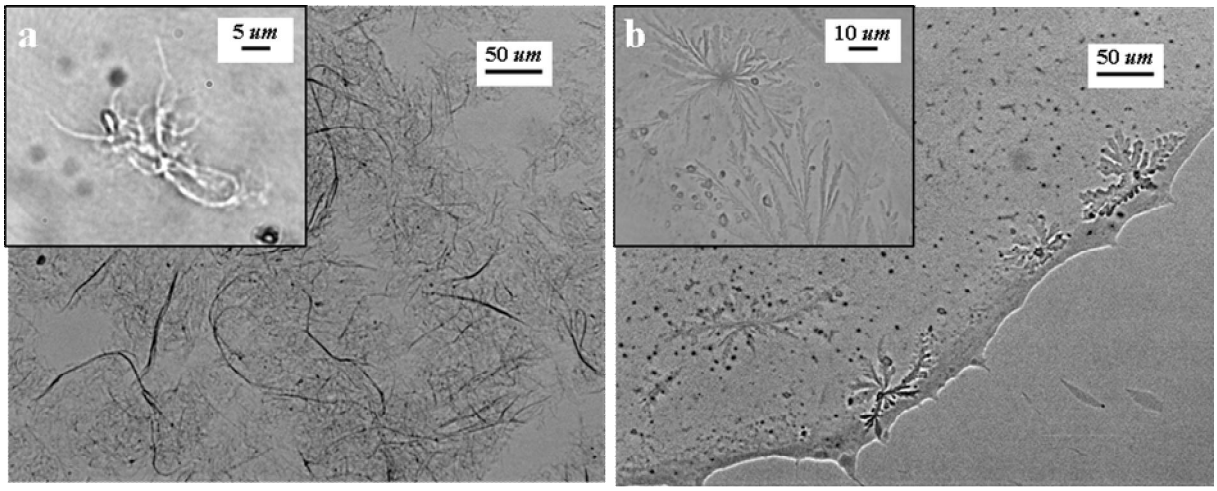

FIGURE 2

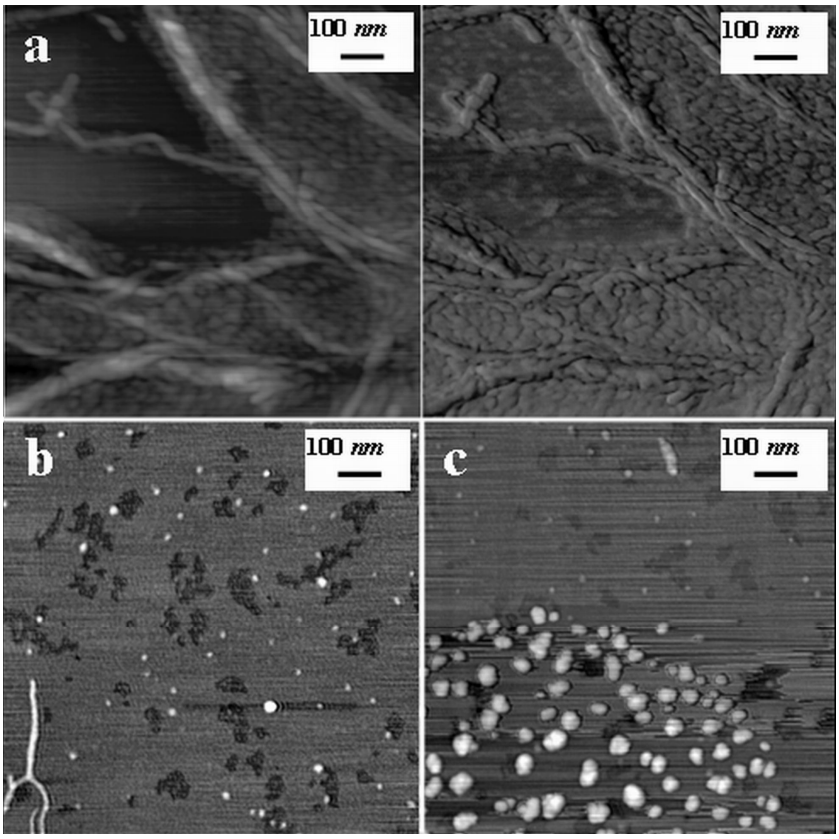

FIGURE 3

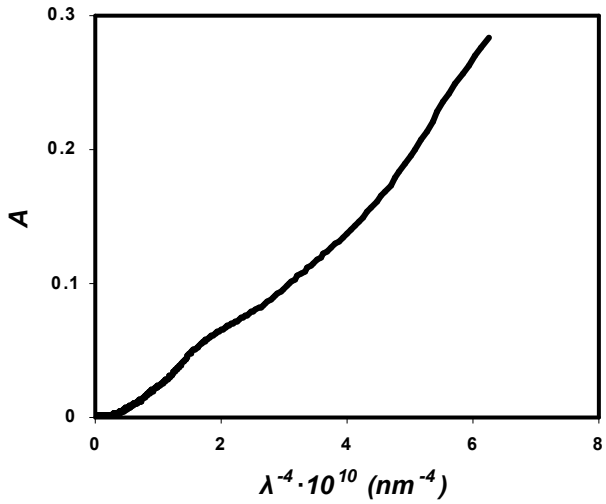

FIGURE 4

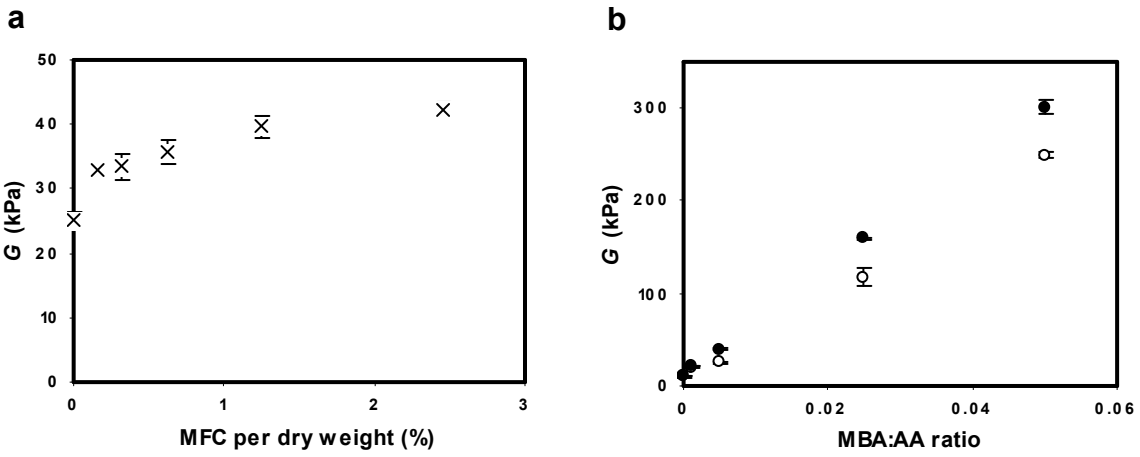

FIGURE 5

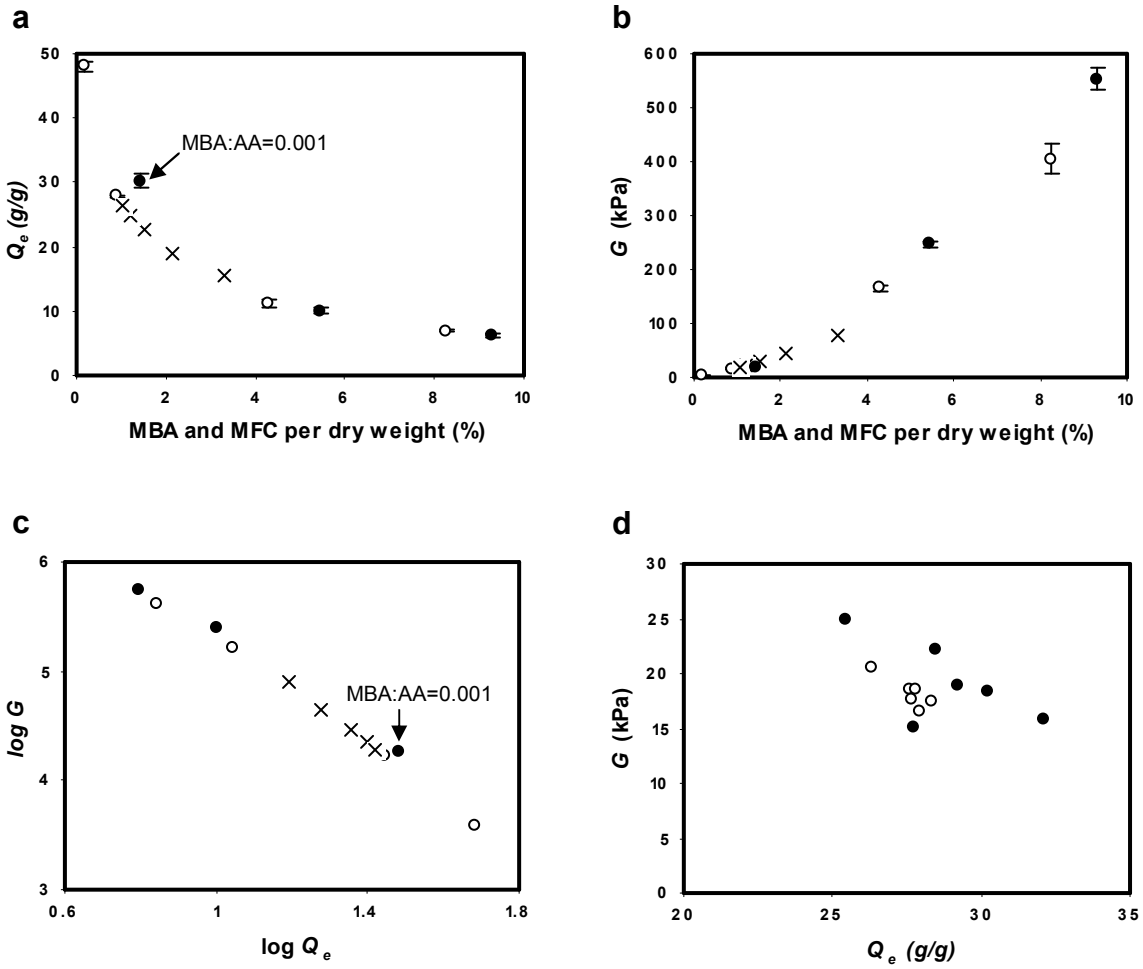
a
MBA:AA=0.001
Q_e (g/g)
MBA and MFC per dry weight (%)
b
G (kPa)
MBA and MFC per dry weight (%)
c
MBA:AA=0.001
log G
log Q_e
d
G (kPa)
Q_e (g/g)

Tables

TABLE 1 Fracture properties of gels after synthesis and after equilibrium swelling. ε_f denotes the strain at fracture, σ_f the compressive strength and G the shear modulus of the gels

Sample	MBA:AA	MFC dry mass %	ε_f	σ_f / kPa	G / kPa
After synthesis[1]					
1	0.05	0	0.37 ± 0.011	298 ± 5.0	249 ± 3.9
2	0.025	0	0.454 ±0.0091	180 ± 17	120 ± 10
3	0.05	1.2	0.377 ± 0.0031	409 ± 7.0	301 ± 7.6
4	0.025	1.2	0.54 ± 0.047	440 ± 78	159.1 ± 0.71
After Swelling[2]					
1	0.05	0	0.21 ± 0.023	190 ± 52	400 ± 27
2	0.025	0	0.34 ± 0.040	170 ± 35	166 ± 6.1
3	0.05	1.2	0.24 ± 0.034	340 ± 55	550 ± 20
4	0.025	1.2	0.32 ± 0.022	220 ± 36	247 ± 5.8

[1] ± indicates min / max values within a synthesis (n = 2)

[2] ± indicates one standard deviation within a synthesis (n = 6)